Extreme Mechanics Letters 40 (2020) 100916

Contents lists available at ScienceDirect

Extreme Mechanics Letters

journal homepage: www.elsevier.com/locate/eml

Highly anisotropic hexagonal lattice material for low frequency water sound insulation

Yi Chen[1], Binghao Zhao[1], Xiaoning Liu, Gengkai Hu *

School of Aerospace Engineering, Beijing Institute of Technology, Beijing 100081, China

ARTICLE INFO

Article history:
Received 23 June 2020
Received in revised form 3 August 2020
Accepted 4 August 2020
Available online 8 August 2020

Keywords:
Anisotropic material
Low impedance
Low frequency
Water sound insulation

ABSTRACT

Insulation of water sound through impedance mismatch has the advantage of broadband effectiveness compared to using materials with bandgaps induced either by local resonance or Bragg scattering. In general, acoustic impedance of an isotropic solid under normal incidence condition is the product of mass density and longitudinal wave velocity. It is derived here, the acoustic impedance of an anisotropic solid depends additionally on a new parameter, and a carefully designed anisotropic solid can achieve a very small impedance along a specific direction. Honeycomb beam lattice is proposed as an example to achieve a much smaller effective impedance than water based on the above principle. Numerical simulation shows, a thin slab, with an overall thickness being two orders of magnitude smaller than the water wavelength, designed from the highly anisotropic lattice can reflect almost 97.7% of incident acoustic energy. A deep subwavelength sample with a thickness 21 mm is then fabricated and measured in a water tube. The experiment shows, the sample can reduce sound transmission by nearly 18.7 dB over the low frequency range 1.5 kHz ∼3.5 kHz. This study demonstrates the potential of anisotropic lattices in engineering effective impedance for insulating water sound at low frequency.

1. Introduction

Insulating water sound is of great value in underwater acoustics engineering, such as reducing noise by drilling equipment, shielding underwater acoustic radiations. Traditionally, insulation relies on impedance mismatch, where larger contrast in impedance leads to higher reflections or insulation [1,2]. Common solids, such as metals or plastics, have impedances being nearly 1000 times larger than air, and can effectively block air sound even with a small thickness. However, the impedance ratios between common solids and water are in the order of 10 due to much larger density of water than air. Therefore, a heavy solid plate with large thickness is unavoidable to block water sound effectively. The situation is even worse when insulating low frequency water sound with larger wavelength.

In the past decades, materials with artificial microstructures, e.g., photonic/phononic crystals and metamaterials, have brought forth many interesting phenomena beyond conventional materials [3–12]. Bandgaps, induced by Bragg scattering or local resonance, are used to prevent acoustic/elastic wave at specific frequency ranges [3]. Bragg bandgaps are due to destructive interferences of waves with comparable wavelength to the lattice period, and usually occur at high frequency ranges. Apart from Bragg scattering, stopping bands can also be formed in sub-wavelength regimes by introduced local resonant elements [13–17]. In such sub-wavelength regimes, the periodic structures behave as metamaterials with effective negative density or negative modulus. They can block wave propagation since only evanescent wave modes are allowed in such single negative materials. However, both mechanisms suffer from a limited bandwidth.

The most feasible design with broadband efficiency returns back to the traditional impedance mismatching. For the case of sound waves normally incident onto an isotropic acoustic medium or elastic solid, only longitudinal wave mode of the medium is excited. Acoustic impedance of the medium is evaluated as the product of mass density and longitudinal wave velocity [2]. To decrease the impedance, one possible solution is reducing the mass density. Air is one such example with its density being nearly 10^3 smaller than water. The impedance of air is thus three orders of magnitude smaller than water, and air is indeed one of the most efficient medium for blocking water sound. However, air suffers from an extremely small modulus due to its very small density, and is not suitable for practical underwater acoustic applications. Nowadays, the design of acoustic material is not limited to isotropic materials. Artificial structures with effective anisotropic elastic properties are frequently employed, and can be easily fabricated with current advanced fabrication technology [18–20]. It is found in this paper

* Corresponding author.
E-mail address: hugeng@bit.edu.cn (G. Hu).
[1] These authors contribute equally.

https://doi.org/10.1016/j.eml.2020.100916
2352-4316/

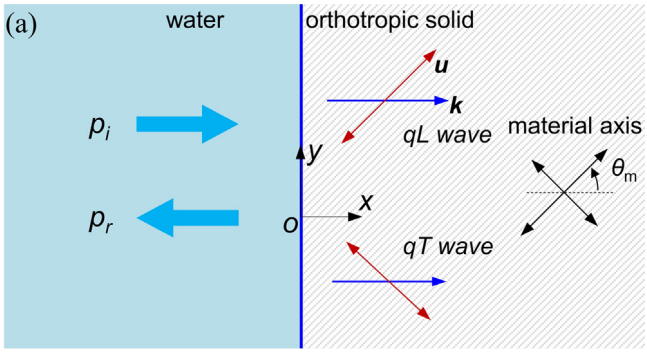

Fig. 1. Transmission and reflection of normally incident acoustic waves onto a water/solid interface. The solid is supposed to be orthotropic, and its material principal direction is orientated at an angle θ_m with respect to the horizontal direction.

that, for the case of sound waves normally incident onto an orthotropic solid, its acoustic impedance differs significantly from that of isotropic case. For general orientation of the principal axis of an orthotropic solid, both quasi-transverse wave and quasi-longitudinal wave are excited simultaneously. The impedance then depends on a new parameter, in addition to the mass density and the quasi-longitudinal wave velocity. The parameter is a function of material anisotropy, orientation of the material as well as the ratio between the quasi-transverse wave velocity and quasi-longitudinal one. This provides us a new degree of freedom to design acoustic impedance as required by using anisotropic microstructure. It will be shown that, an extremely small impedance can be achieved by tailoring the anisotropic microstructure, while the mass density and the wave velocity are not necessarily very small. This finding enables us to design anisotropic microstructures with small impedance compared to water, and to explore prominent sound insulation behavior with such solids.

This article is organized as follows. We first investigate acoustic transmission between water and an anisotropic solid, and derive the conditions for obtaining low impedance. The derived conditions are verified through sound insulation performance of a slab with pre-assumed anisotropic material property. Secondly, we propose a honeycomb beam lattice as example for realizing the small effective impedance through microstructure design. Numerical simulations are carried out to validate the impedance design and its sound insulation behavior. Thirdly, experimental sample based on the honeycomb beam lattice is fabricated and experimentally tested in a water acoustic tube to demonstrate its sound insulation performance at low frequency range. Finally follows a brief summary.

2. Theory of sound insulation with anisotropic solids

We study the acoustic transmission of a plane wave normally incident onto an interface separating water and a solid (Fig. 1). We assume a mass density $\rho_0 = 1000\ \mathrm{kg/m^3}$ and a sound velocity $c_0 = 1500\ \mathrm{m/s}$ for water. The solid material is supposed to be orthotropic, and its material principal axis shows an angle θ_m with respect to horizontal direction. For the case of aligned principal axis to the interface, i.e., $\theta_m = 0°$ or 90°, a normally incident plane wave only excites purely longitudinal wave mode in the solid. For the other angles $\theta_m \neq 0°$ and 90°, both quasi-longitudinal wave mode (qL mode) and quasi-transverse wave mode (qT mode) will be excited. One should notice here, a purely longitudinal wave mode or transverse wave mode exists only along the principal axes of the orthotropic solid.

To derive the reflected pressure, we need to solve the two wave modes in the solid. For the considered normally incident plane waves, wave vector of the excited wave mode is along $+x$ direction. Therefore, displacement fields of the two modes are $\mathbf{u} = \mathbf{u}_0 \exp(ikx)$, with k being the wave number and $\mathbf{u}_0 = \{u_0, v_0\}$ the displacement polarization. The time harmonic term, $\exp(-i\omega t)$ with ω being the circular frequency is omitted. The mass density of the orthotropic solid is assumed to be ρ_s and the two-dimensional constitutive law in a global coordinate xoy reads,

$$\begin{pmatrix}\sigma_x\\ \sigma_y\\ \sigma_{xy}\end{pmatrix} = \begin{pmatrix}C_{11} & C_{12} & C_{16}\\ C_{12} & C_{22} & C_{26}\\ C_{16} & C_{26} & C_{66}\end{pmatrix}\begin{pmatrix}\varepsilon_x\\ \varepsilon_y\\ \gamma_{xy}\end{pmatrix}, \tag{1}$$

where, σ_x, σ_y and σ_{xy} are the stress and, ε_x, ε_y and γ_{xy} are the engineering strain, respectively. By substituting the above displacement fields into the dynamic elasticity equation $-\omega^2\rho_s\mathbf{u} = \nabla\cdot\boldsymbol{\sigma}$, and the following eigenvalue problem is derived,

$$\begin{pmatrix}C_{11}k^2-\rho_s\omega^2 & C_{16}k^2\\ C_{16}k^2 & C_{66}k^2-\rho_s\omega^2\end{pmatrix}\begin{pmatrix}u_0\\ v_0\end{pmatrix} = 0. \tag{2}$$

This equation has two non-trivial solutions, one corresponding to the qL mode and the other to qT mode. Displacement fields for the qL mode and qT mode are, respectively,

$$\mathbf{u}_{qL} = \{1, \tan\theta_{qL}\}\exp(ik_{qL}x) \tag{3}$$

$$\mathbf{u}_{qT} = \{1, \tan\theta_{qT}\}\exp(ik_{qT}x) \tag{4}$$

$$c_{qL} = \sqrt{\frac{C_{11}+C_{66}+\sqrt{\Delta}}{2\rho_s}},\quad \theta_{qL} = \tan^{-1}\frac{2C_{16}}{C_{11}-C_{66}+\sqrt{\Delta}} \tag{5}$$

$$c_{qS} = \sqrt{\frac{C_{11}+C_{66}-\sqrt{\Delta}}{2\rho_s}},\quad \theta_{qS} = \tan^{-1}\frac{2C_{16}}{C_{11}-C_{66}-\sqrt{\Delta}}, \tag{6}$$

in which, $k_{qL} = \omega/c_{qL}$ and $k_{qT} = \omega/c_{qT}$ are respectively the wave numbers of the qL mode and qT mode, c_{qL} and c_{qT} are the wave velocities, and $\Delta = 4(C_{16})^2 + (C_{11}-C_{66})^2$. θ_{qL} and θ_{qT} are the polarization angles, i.e., the angle between the vibration direction of material particles and the wave vector, corresponding to the qL mode and qT mode, respectively. The qL mode is closer to longitudinal mode since θ_{qL} is smaller than 45°. The two modes become purely longitudinal ($\theta_{qL} = 0°$) or transversal ($\theta_{qT} = 90°$) only if the material axis is parallel to the interface as mentioned previously. For isotropic cases, the two modes are always purely longitudinal and transversal.

Now we write the total pressure in water as

$$p_1 = p_i\exp(ik_0x) + p_r\exp(-ik_0x), \tag{7}$$

in which p_i denotes the amplitude of the incident wave, and $k_0 = \omega/c_0$ is the wave number in water. For inclined material principal axis, both the qL and qT modes in the solid will be excited. Displacement fields in the solid is of the form $\mathbf{u} = t_{qL}\mathbf{u}_{qL} + t_{qT}\mathbf{u}_{qT}$,

$$\begin{cases} u = t_{qT}\exp(ik_{qT}x) + t_{qL}\exp(ik_{qL}x)\\ v = t_{qT}\tan\theta_{qT}\exp(ik_{qT}x) + t_{qL}\tan\theta_{qL}\exp(ik_{qL}x)\end{cases}. \tag{8}$$

t_{qL} and t_{qT} are the transmittance coefficient for the qL mode and qT mode, respectively. By considering the continuous condition for the normal displacement and the surface traction at the water/solid interface, the following reflection coefficient is obtained,

$$R = \frac{p_r}{p_i} = \frac{Z-\rho_0c_0}{Z+\rho_0c_0} \tag{9}$$

where

$$Z = \eta \rho_s c_{qL}, \quad \eta = \frac{1 + \tan^2 \theta_{qL}}{1 + \left(c_{qL}/c_{qT}\right) \tan^2 \theta_{qL}}. \tag{10}$$

Eq. (9) is the same as acoustic reflection between two fluids. Therefore, one can consider Z as an effective acoustic impedance of the solid. This effective acoustic impedance, Eq. (10), is valid for both isotropic solids and anisotropic solids. For an isotropic solid, the factor η is fixed to be $\eta = 1$ since $\tan\theta_{qL} = 0$, and the impedance depends only on the density ρ_s and the longitudinal wave c_{qL} as expected. For an anisotropic solid, the parameter η provides a new degree of freedom to tune the effective impedance Z.

In order to achieve a high reflection for water sound, a much larger impedance or a much smaller impedance than water is needed. Higher impedance requires a much larger density or a much larger sound velocity than water, which is hardly possible with common solids. Usually, a very thick solid plate is required to insulate water sound efficiently. For instance, in order to insulate 90% energy of incident plane underwater acoustic waves at 2 kHz, a steel plate with a thickness as large as 93 mm, or with an area density 730 kg/m^2, is unavoidable or an aluminum plate with an even large thickness 299 mm and an area density 800 kg/m^2 is required. An alternative strategy to block water sound is to use materials with much smaller impedance than water. Air is one example, and its impedance is three orders of magnitude smaller than water because its mass density is three orders of magnitude smaller. However, the extremely low density of air also results in its very small modulus, and this limits its practical applications in underwater environment. Here, as shown in Eq. (10), by designing anisotropic material with an extremely small factor η, it is possible to realize much smaller impedance than water while the effective mass density is not necessarily small. From Eq. (10), an extremely small $\eta << 1$ implies the following three conditions:

(1) The anisotropy is necessary,

(2) The material principal axes are oblique to the interface, $\theta_m \neq 0$ or 90°,

(3) The quasi-transverse wave velocity is much smaller than the quasi-longitudinal one, i.e. $c_{qL}/c_{qT} >> 1$.

The conditions (1) and (2) together ensure $\tan\theta_{qL} \neq 0$. To figure out what kind of orthotropic solids can achieve very small impedance, we consider the following elasticity matrix in the principal coordinate system,

$$\mathbf{C} = \begin{pmatrix} C^0_{11} & C^0_{12} & 0 \\ C^0_{12} & C^0_{22} & 0 \\ 0 & 0 & C^0_{66} \end{pmatrix} = \begin{pmatrix} \Lambda^{-1} & \nu & 0 \\ \nu & \Lambda & 0 \\ 0 & 0 & \mu \end{pmatrix} K_C \tag{11}$$

in which

$$\Lambda = \sqrt{\frac{C^0_{22}}{C^0_{11}}}, \quad \nu = \frac{C^0_{12}}{\sqrt{C^0_{11} C^0_{22}}}, \quad \mu = \frac{C^0_{66}}{\sqrt{C^0_{11} C^0_{22}}}, \quad K_C = \sqrt{C^0_{11} C^0_{22}}. \tag{12}$$

The material anisotropy is partially determined by Λ. ν and μ are two parameters related to easy deformation modes [21]. If the parameter ν is close to 1 and the parameter μ is very small, the material is called a bi-mode material, or a two-dimensional pentamode material [22]. In such materials, the quasi-transverse wave velocity is much smaller than the quasi-longitudinal wave velocity. Therefore, the bi-mode material is one possible choice to achieve extremely small impedance.

In the following plots, we consider five combinations for the parameter group (ν, μ). We set the anisotropy $\Lambda = 5$, and set ρ_s and K_c to be the density and bulk modulus of water, $\rho_s = \rho_0$ and $K_c = K_0 = 2.25$ GPa, respectively. The effective acoustic impedance, normalized by that of water $Z_0 = \rho_0 c_0$, is plotted in Fig. 2 as a function of the material orientation angle θ_m. It can be easily seen that, the achievable minimum impedance is mainly determined by the parameter ν, while the other parameter μ determines the range of θ_m available for small impedance. Therefore, at least the parameter ν of the material should be close to 1 to achieve a small impedance. Indeed, these materials can be understood as uni-mode materials [22]. The anisotropic factor Λ determines the angle, $\theta_{min} = \cos^{-1}\sqrt{\Lambda/(1+\Lambda)}$, for which the minimal impedance is achieved. We also plot in Fig. 2(a) and (b) the Young's modulus E as a function of the orientation angle θ_m. It is interesting to note that, for the case with the parameter ν close to 1 (Fig. 1(a)), when the acoustic impedance reaches the minimal, the Young's modulus E is not necessarily minimal. Despite the above derived impedance is for normal incidence condition, it will be shown in the following that, highly reflection is also preserved for oblique incidence.

To verify the above impedance analysis, we study acoustic transmission of a solid plate under normal and oblique plane wave incidences (Fig. 3). Sound reduction index (SRI) is used to characterize the sound insulation performance, and is obtained as $-20\log_{10}|T|$ with T being the transmission coefficient. We choose the above material parameters, $\rho_s = \rho_0$, $K_c = K_0$, $\Lambda = 5$, $\nu = 0.999$ and $\mu = 0.001$ for the solid plate. When the material principal direction is aligned with the interface, i.e., $\theta_m = 0°$, 90° the acoustic impedance is comparable to that of water $Z(\theta_m = 0°) = 0.45Z_0$, $Z(\theta_m = 90°) = 2.24Z_0$. For the studied low frequency range $fd/c_0 = 0.05$, or equivalently $\lambda = c_0/f > 20d$, the corresponding SRI in Fig. 3(b) is less than 1 dB for incident angles smaller than 30°. If the material axis is chosen to be $\theta_m = 28.5°$, the acoustic impedance becomes much smaller $Z(\theta_m = 28.5°) = 0.0385Z_0$. The calculated results in Fig. 3(c) indicate a highly reflective behavior, and the SRI is larger than 20 dB for most incident angles and frequency. For instance, a 20 dB reduction in transmission is achieved at a very low frequency $f = 0.0025c_0/d$. This means, 99% of the incident energy is reflected by the plate, although the plate is extremely thin compared to the wavelength $\lambda = 400d$. It is noted that, the horizontal bright blue lines in Fig. 3(c) denotes Fabry–Perot resonant transmission. The resonances are attributed to shear waves in the plate [23]. They occur at very low frequencies due to the extremely small shear wave velocity.

3. Microstructure design and numerical validation

The above investigations are all based on hypothetical material parameters. Here, we will implement the low impedance by using honeycomb beam lattice (Fig. 4(a)). The lattice can be treated as a bi-mode material when the beams are sufficient thin, and the corresponding parameter ν and μ are respectively close to 1 and 0 [21]. We remark here that; the honeycomb lattice is not the only choice. Indeed, from the previous analysis, lattices with only the parameter ν being close to 1 can be used to achieve low impedance.

The honeycomb beam lattice is characterized by three dimensionless parameters, i.e. the length ratio h/l, the dimensionless beam thickness t/l and the topology angle β (Fig. 4(a)). The lattice is isotropic when $h = l$ and $\beta = 60°$, otherwise becomes anisotropic. All the beams are assumed to be composed of aluminum with mass density $\rho_{Al} = 2700$ kg/m^3, Young's modulus $E_{Al} = 69$ GPa and Poisson's ratio $\nu_{Al} = 0.33$. Plane waves normally incident onto the lattice from the left, as indicated by black arrows (Fig. 4(a)). We first study the achievable effective properties' range of the honeycomb beam lattice. For

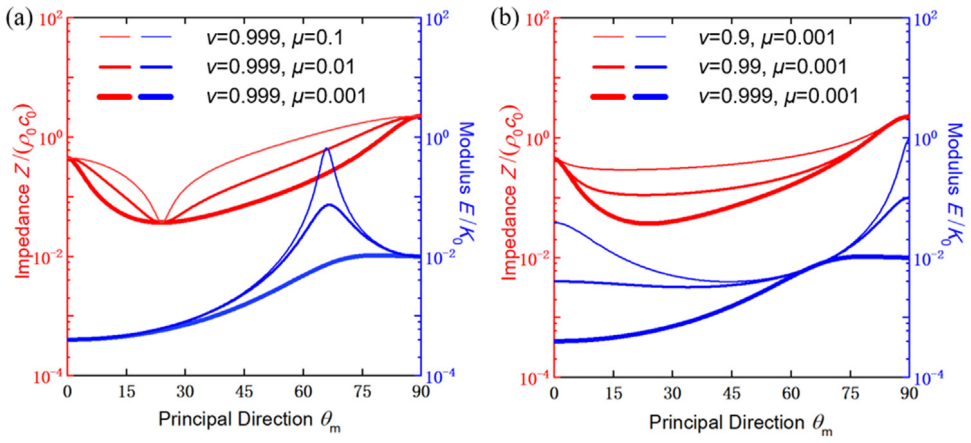

Fig. 2. Normalized effective acoustic impedance and Young's modulus of orthotropic solids versus different material principal direction θ_m. Impedance is calculated from Eq. (10).

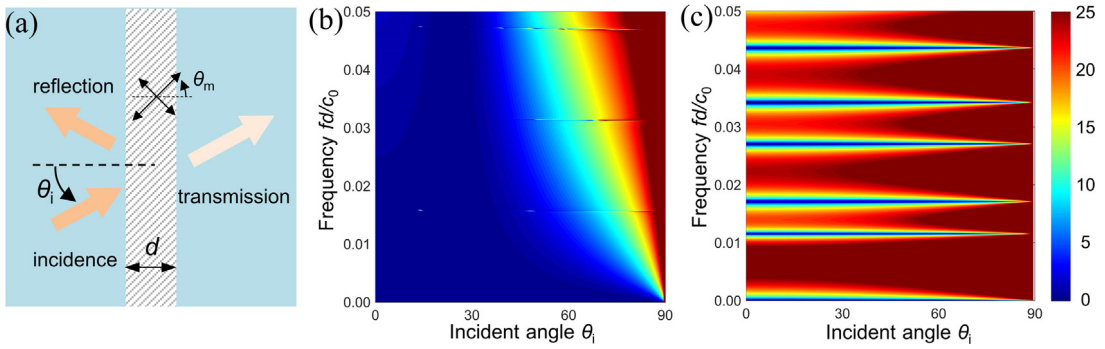

Fig. 3. (a) Sketch of acoustic transmission through solid plate. Material parameters of the solid plate are $\rho_s = \rho_0$, $K_c = K_0$, $\Lambda = 5$, $\nu = 0.999$ and $\mu = 0.001$. θ_m indicates the material orientation angle, and θ_i indicates the incidence angle. (b) Calculated SRI versus normalized wave frequency fd/c_0 and the incidence angle θ_i; Principal direction of the solid is parallel with the interface $\theta_m = 0°$; (c) The same as in (b) but for $\theta_m = 28.5°$. (For interpretation of the references to color in this figure legend, the reader is referred to the web version of this article.)

the geometry parameters $60° \le \beta \le 80°$, $0.25 \le h/l \le 1.0$, $0.03 \le t/l \le 0.2$, and the lattice orientation angle $0 \le \theta_m \le 90$, Fig. 4(b) shows the attainable effective impedance and the effective mass density. Here, the effective material parameters are retrieved based on dispersion relations [21]. The black curve is for isotropic lattice with $\beta = 60°$ and $h/l = 1.0$, where the effective mass density and the effective impedance follows a power law $Z \sim \rho^2$. For anisotropic lattices with orientation angle $\theta_m = 0°$, the achievable range of the effective impedance and the mass density is as indicated by the pink region. If we allow for rotated lattice axis, i.e., $\theta_m \neq 90°$, the achievable properties cover a larger space. The available small effective impedance can be further decreased by an order of magnitude. Apparently, for the same effective mass density, we have a much broader design space for the effective impedance by taking into account of anisotropy and lattice orientation, and particularly can achieve much smaller effective impedance.

We compare here an isotropic lattice ($\beta = 60°$, $h/l = 1.0$ and $t/l = 0.059$) and an anisotropic lattice ($\beta = 74°$, $h/l = 0.25$ and $t/l = 0.03$). The two lattices share the same effective density $\rho_s = 0.179\rho_0$. Effective elasticity parameters of the isotropic lattice are $C^0_{11} = C^0_{22} = 0.601K_0$, $C^0_{12} = 0.593K_0$, and $C^0_{66} = 0.004K_0$, and those of the anisotropic lattice are $C^0_{11} = 0.041K_0$, $C^0_{22} = 1.718K_0$, $C^0_{12} = 0.264K_0$ and $C^0_{66} = 0.006K_0$. Although the two lattices share the same porosity, their effective impedances are much different. The effective impedance of the anisotropic lattice without rotating the material axis (marked as **B** in Fig. 4(b)) is smaller than the isotropic one (marked as **A** in Fig. 4(b)). Furthermore, by choosing a lattice orientation angle $\theta_m = 28.5°$, the effective impedance (marked as **C** in Fig. 4(b)) is further decreased. We show in Fig. 4(c) the simulated SRI of the slabs with microstructures corresponding to the **A**, **B** and **C** cases. The simulations are performed using coupled acoustic-solid module in COMSOL Multiphysics. Voids in the structures are filled with air ($\rho_{air} = 1.29$ kg/m^3, $c_{air} = 343$ m/s), and the background region is occupied by water ($\rho_0 = 1000$ kg/m^3, $c_0 = 1500$ m/s). The plate thickness is $d = 21$ mm. For the studied frequency range 0.1 kHz $\le f \le$ 3.5 kHz, or equivalently $20d \le \lambda \le 700d$, the isotropic lattice (case **A**) is nearly transparent to water sound. The anisotropic lattice without rotating the material axis (case **B**) has a moderate insulation at high frequency range. For a rotated material axis $\theta_m = 28.5°$ (case **C**), the anisotropic lattice shows obvious sound insulation over the entire studied frequency range. For instance, at a frequency 238 Hz (see arrow in Fig. 4(c)), despite the wavelength is 300 times larger than the plate $\lambda = 300d$, the lattice can block nearly 97.7% of the incident energy with an SRI 16.4 dB. The sharp drop of sound insulation for case **C** in Fig. 4(c) at around 3 kHz is also due to Fabry–Perot resonance transmission, the same as in Fig. 3(c).

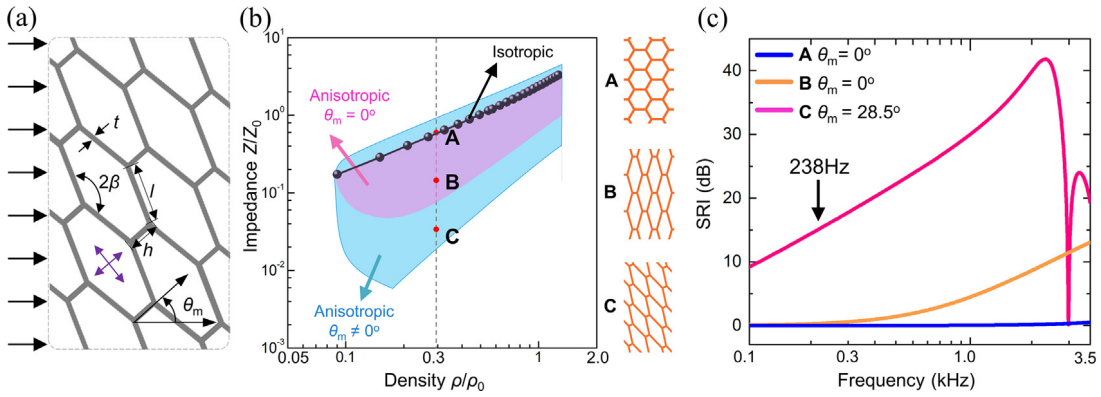

Fig. 4. (a) Honeycomb lattice composed of beams with thickness t, length h and l and topology angle β. The lattice orientation forms an angle θ_m with respect to horizontal direction; (b) Attainable effective impedance and effective mass density of the lattice with the geometry parameters $60° \leq \beta \leq 80°$, $0.25 \leq h/l \leq 1.0$, $0.03 \leq t/l \leq 0.2$, and the orientation angle $0 \leq \theta_m \leq 90$; (c) Numerically simulated SRI for slabs composed of isotropic and anisotropic lattices, respectively.

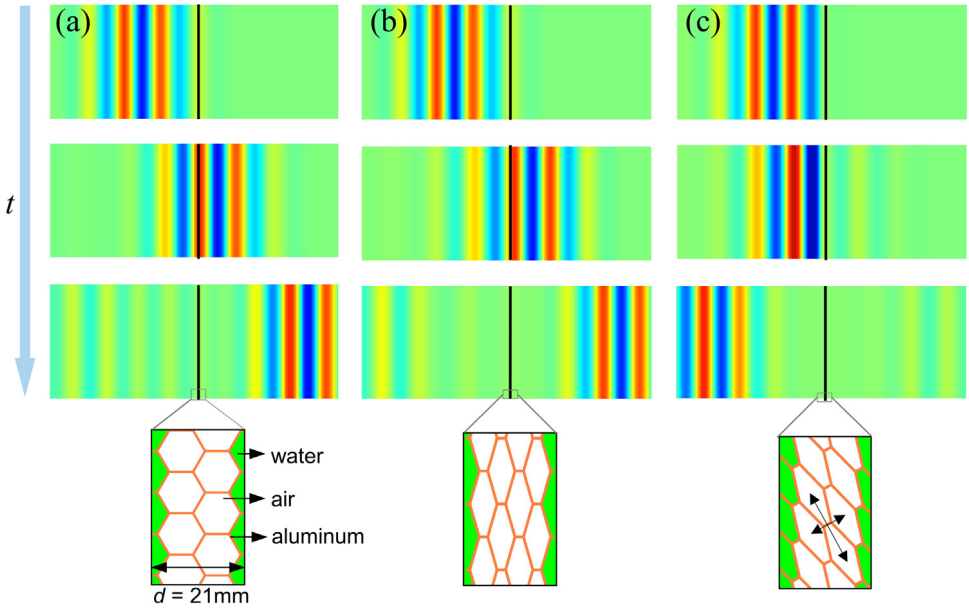

Fig. 5. (a) Simulated pressure fields for transient plane waves incident onto a microstructured slab assembled from isotropic lattice (case A in Fig. 4(b)) at different time. (b) (c) The same as in (a) but for anisotropic lattice without rotating the principal direction (case B in Fig. 4(b)), and with rotated principal direction (case C in Fig. 4(b)), respectively.

Furthermore, we simulate the transient response of the three microstructured slabs under the incidence of a Gaussian pulse $\exp(-(\pi t/3000)^2) \times \cos(2\pi f_c t)$, with a central frequency $f_c = 238$ Hz. The Gaussian pulse lasts for about two periods $t = 2/f_c = 8.4$ ms, and has a half-amplitude width 143 Hz. As expected, the incident wave completely transmits through the slab composed of the isotropic lattice (Fig. 5(a)). For the slab corresponding to the anisotropic lattice without rotating the material axis (Fig. 5(b)), the result is similar due to the significant large wavelength compared to the slab $\lambda = 300d$. However, once the anisotropic lattice is rotated, the corresponding slab almost totally reflects the incident wave (Fig. 5(c)). Since all the three lattices have the same porosity, one can conclude that, both the anisotropy and the rotated material axis are necessary in reducing the effective impedance of the lattice.

4. Experiment verification

Finally, we experimentally verify the proposed water sound insulation design by using the above honeycomb beam lattice. The experiment sample is composed of anisotropic beam lattice with the same geometry parameter as in Case **C** ($\beta = 60°$, $h/l = 0.25$, and $l = 10$ mm), except for that a larger beam thickness $t/l = 0.05$ is used instead. Thicker beams reduce the insulation performance, however facilitate the fabrication. A circular microstructure slab (see inset of Fig. 6(a)) is fabricated using the advance electric discharging machining technology with an accuracy tolerance 0.02 mm. The sample has a diameter 200 mm and a thickness 21 mm, and is sealed with a 2-mm-thick rubber to prevent water from entering into the void. The principal axis of the lattice is also chosen as $\theta_m = 28.5°$. The effective acoustic impedance of the lattice is 2 orders of magnitude smaller than that of water, $Z_{eff} = 0.0536Z_0$. The sample is sandwiched in

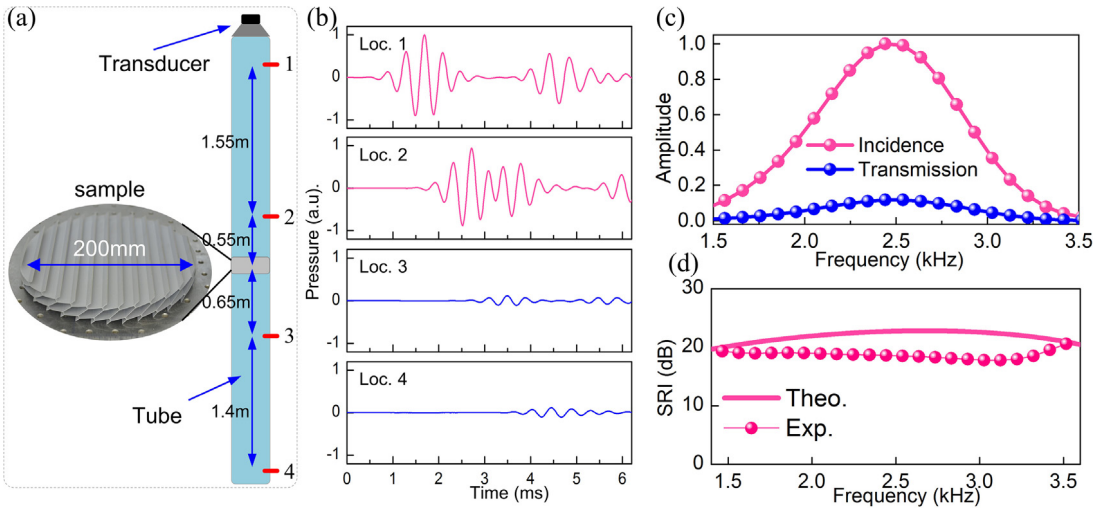

Fig. 6. (a) Fabricated aluminum sample and setup for the underwater sound transmission experiment; Underwater sound wave is generated by a transducer at the top and pressure signals at the four marked locations are measured by hydrophones; (b) Measured transient acoustic signals at the four locations; (c) Fourier transformed amplitude for incident signal at location 1 and transmitted signal at location 3. (d) SRI evaluated from the incident and transmitted signals.

the middle of a water tube (Fig. 6(a)). Transient acoustic waves incident onto the sample from the top end, and pressures at the four indicated locations are measured.

The incident wave is also a Gaussian pulse as in the numerical simulation. Due to the frequency limitation of the experiment system, the central frequency of the Gaussian pulse is 2.5 kHz. The measured signals at the four locations are shown in Fig. 6(b). From the measured signals at the backward locations (Loc.1 and Loc. 2), the reflective signals after the incident wave are clearly observed, and their amplitudes are slightly weaker than the incident ones. Due to a short distance of the measured position to the sample, reflected pulse at positions 2 partially overlaps with the incident one. For the forward locations 3 and 4, the transmitted signals are much weaker than the incident ones as expected. To quantify the SRI, we perform Fourier transformation to the incident pulse at position 1 and transmitted one at position 3. The central frequency is clearly around 2.5 kHz, and a half amplitude width extends from 1.5 kHz to 3.5 kHz is observed (Fig. 6(c)). The SRI is obtained as $-20\times\mathrm{Log}_{10}(A_T/A_I)$, where A_T/A_I represents the Fourier transformed amplitude of the transmitted and incident wave packet. The measured SRI is nearly 18.7 dB in average over the frequency range. The result indicates a very prominent insulation performance of the microstructure slab. In addition, the measurement agrees very well with theory based on homogenized material properties.

5. Conclusions

Through theoretical analysis of acoustic transmission between water and anisotropic solids, we find that, the effective impedance of anisotropic solids can be tailored by a new parameter in addition to the mass density and the quasi-longitudinal wave velocity. Therefore, by tuning this parameter, we proposed to realize anisotropic solids with extremely small impedance and applied them to insulate low frequency water sound. To obtain extremely small impedance, the material should be highly anisotropy and the material principal direction should be oblique with respect to the interface, and most importantly the quasi-transverse wave velocity should be as small as possible compared to the quasi-longitudinal one. The above design principles have been verified by using pre-assumed continuum anisotropic materials and actual honeycomb lattice. Furthermore, a microstructured slab based on highly anisotropic honeycomb beam lattice is fabricated, and experiment is carried out to verify the designed sound insulation behavior. The measurement shows an average of sound reduction index 18.7 dB for incident water sound at the low frequency range 1.5 kHz to 3.5 kHz. This study provides a novel strategy to the design acoustic impedance from highly anisotropic solids.

Declaration of competing interest

The authors declare that they have no known competing financial interests or personal relationships that could have appeared to influence the work reported in this paper.

Acknowledgments

This work was supported by the National Natural Science Foundation of China (Nos. 11472044, 11632003, 11802017, 11991030, 11991033), and Beijing Science and Technology Commission, China (No. Z191100004819003).

References

[1] J. Marage, Y. Mori, M. Kutz, Sonars and Underwater Acoustics, Wiley Online Library, 2013.
[2] L.E. Kinsler, A.R. Frey, A.B. Coppens, J.V. Sanders, Fundamentals of Acoustics, Wiley, 1999.
[3] M.S. Kushwaha, P. Halevi, G. Martinez, L. Dobrzynski, B. Djafari-Rouhani, Theory of acoustic band structure of periodic elastic composites, Phys. Rev. B 49 (1994) 4.
[4] Z.Y. Liu, X.X. Zhang, Y.W. Mao, Y. Zhu, Z.Y. Yang, C.T. Chan, P. Sheng, Locally resonant sonic materials, Science 289 (2000) 5485.
[5] A.N. Norris, Acoustic metafluids, J. Acoust. Soc. Am. 125 (2009).
[6] X.N. Liu, G.K. Hu, C.T. Sun, G.L. Huang, Wave propagation characterization and design of two-dimensional elastic chiral metacomposite, J. Sound Vib. 330 (2011) 11.
[7] A.N. Norris, A.J. Nagy, Metal water: A metamaterial for acoustic cloaking, in: Proceedings of Phononics, Santa Fe, New Mexico, USA, 2011.
[8] R. Zhu, X.N. Liu, G.K. Hu, C.T. Sun, G.L. Huang, Negative refraction of elastic waves at the deep-subwavelength scale in a single-phase metamaterial, Nature Commun. 5 (2014).
[9] Y. Chen, M. Zheng, X. Liu, Y. Bi, Z. Sun, P. Xiang, J. Yang, G. Hu, Broadband solid cloak for underwater acoustics, Phys. Rev. B 95 (2017) 180104.

[10] X. Su, A.N. Norris, C.W. Cushing, M.R. Haberman, P.S. Wilson, Broadband focusing of underwater sound using a transparent pentamode lens, J. Acoust. Soc. Am. 141 (2017) 6.
[11] Z. Sun, X. Sun, H. Jia, Y. Bi, J. Yang, Quasi-isotropic underwater acoustic carpet cloak based on latticed pentamode metafluid, Appl. Phys. Lett. 114 (2019) 9.
[12] Z. Sun, H. Jia, Y. Chen, Z. Wang, J. Yang, Design of an underwater acoustic bend by pentamode metafluid, J. Acoust. Soc. Am. 3 (2018) 142.
[13] J. Li, C.T. Chan, Double-negative acoustic metamaterial, Phys. Rev. E 70 (2004) 5.
[14] Z.Y. Liu, C.T. Chan, P. Sheng, Analytic model of phononic crystals with local resonances, Phys. Rev. B 71 (2005) 0141031.
[15] M.H. Lu, C. Zhang, L. Feng, J. Zhao, Y.F. Chen, Y.W. Mao, J. Zi, Y.Y. Zhu, S.N. Zhu, N.B. Ming, Negative birefraction of acoustic waves in a sonic crystal, Nature Mater. 6 (2007) 10.
[16] Yao S., Zhou X., Hu G., Experimental study on negative effective mass in a 1D mass–spring system, New. J. Phys. 10 (2008) 043020.
[17] X.M. Zhou, G.K. Hu, Analytic model of elastic metamaterials with local resonances, Phys. Rev. B 79 (2009) 19.
[18] J. Christensen, F.J.G. de Abajo, Anisotropic metamaterials for full control of acoustic waves, Phys. Rev. Lett. 108 (2012) 12.
[19] M. Kadic, T. Bückmann, R. Schittny, M. Wegener, On anisotropic versions of three-dimensional pentamode metamaterials, New J. Phys. 15 (2013) 023029.
[20] B.I. Popa, W. Wang, A. Konneker, S.A. Cummer, C.A. Rohde, Anisotropic acoustic metafluid for underwater operation, J. Acoust. Soc. Am. 139 (2016) 6.
[21] Y. Chen, X.N. Liu, G.K. Hu, Latticed pentamode acoustic cloak, Sci. Rep-Uk 5 (2015).
[22] G.W. Milton, A.V. Cherkaev, Which elasticity tensors are realizable? J. Eng. Mater. Technol. 117 (1995) 4.
[23] Y. Chen, X. Liu, G. Hu, Influences of imperfectness and inner constraints on an acoustic cloak with unideal pentamode materials, J. Sound Vib. 458 (2019) 13.